Richman, J. B. Y., & Verpoorte, J. A. (1981) *Can. J. Biochem. 59*, 519–523.
Salomon, D. S., Bano, M., Smith, K. B., & Kidwell, W. R. (1982) *J. Biol. Chem. 257*, 14093–14101.
Salvesen, G. S., Sayers, C. A., & Barrett, A. J. (1981) *Biochem. J. 195*, 453–461.
Straight, D. L., & McKee, F. A. (1982) *Biochemistry 21*, 4550–4555.
Swenson, R. P., & Howard, J. B. (1979a) *J. Biol. Chem. 254*, 4452–4456.
Swenson, R. P., & Howard, J. B. (1979b) *Proc. Natl. Acad. Sci. U.S.A. 76*, 4313–4316.
Swenson, R. P., & Howard, J. B. (1980) *J. Biol. Chem. 255*, 8087–8091.
Tack, B. F., Janatova, J., Thomas, M. L., Harrison, R. A., & Hammer, C. H. (1981) *Methods Enzymol. 80*, 64–101.
Teller, D. C., Swanson, E., & de Haen, C. (1979) *Methods Enzymol. 61*, 103–124.
Thomas, M. L., Janatova, J., Gray, W. R., & Tack, B. F. (1982) *Proc. Natl. Acad. Sci. U.S.A. 79*, 1054–1058.
Van Leuven, F., Cassiman, J.-J., & Van den Berghe, H. (1978) *Exp. Cell Res. 117*, 273–282.
Van Leuven, F., Cassiman, J.-J., & Van den Berghe, H. (1979) *J. Biol. Chem. 254*, 5155–5160.
Van Leuven, F., Cassiman, J.-J., & Van den Berghe, H. (1981) *J. Biol. Chem. 256*, 9016–9022.
Van Leuven, F., Cassiman, J.-J., & Van den Berghe, H. (1982) *Biochem. J. 201*, 119–128.

Mechanism of Adenosinetriphosphatase Activity of Trinitrophenylated Myosin Subfragment 1†

Andras Muhlrad*

ABSTRACT: The rate and extent of conformational changes induced by nucleotides in trinitrophenylated myosin subfragment 1 (S-1) were studied. The absorbance spectrum of the trinitrophenyl moiety attached to the reactive lysyl residue of S-1 changed considerably upon addition of ATP or its analogues. ATP or AMP-PNP induced a larger spectral change than that of ADP, and its value was independent of the presence of Mg^{2+}. The trinitrophenylation of the reactive lysine considerably decreased the enhancement of the tryptophan fluorescence induced by MgATP, while it did not affect fluorescence enhancement induced by MgADP or MgAMP-PNP. The rate of formation of nucleotide-induced absorbance changes in trinitrophenylated (TNP) S-1 was followed in a stopped-flow spectrophotometer. The reaction could be described by a single exponential at every nucleotide concentration. The calculated apparent first-order rate constant, k_{obsd}, increased with rising concentrations of MgATP, ATP, MgADP, and MgAMP-PNP and finally reached a plateau. The absorbance change that appeared upon addition of MgATP to TNP S-1 eventually decayed in two phases until it reached the level of that induced by MgADP. The nucleotide concentration dependence of k_{obsd} deviated from a hyperbolic function in all cases studied. The nucleotide concentration dependence of the signal amplitude was also measured, and it was found to be independent of the presence of Mg^{2+}. The obtained results deviated from a computer-simulated binding curve, which was computed by assuming one identical binding site for each TNP S-1 molecule. The results indicate that an enzyme–substrate complex is the predominant intermediate in the TNP S-1 catalyzed MgATP hydrolysis, instead of an enzyme–product complex, which is the case with normal, unmodified S-1.

Myosin subfragment 1 (S-1)[1] is the segment of the myosin molecule responsible for ATPase activity and interaction with actin. A major effort was made in recent years to describe the molecular mechanism of ATP hydrolysis catalyzed by S-1, as well as the localized conformational changes coupled with the reaction. Several results pointed to localized conformational changes that are induced in myosin on addition of ATP or its analogues and on hydrolysis of the substrate. Changes were detected in the fluorescence intensity of 8-anilino-1-naphthalenesulfonate (ANS) bound to myosin (Cheung, 1969), in the environment of tryptophanyl residues, as indicated by ultraviolet (Morita, 1967) and fluorescence difference spectra (Werber et al., 1972) and in the ESR spectrum of spin-labels attached to the SH_1 thiol (Seidel et al., 1970). The conformation of the junction between the 27K and 50K fragments of S-1's heavy chain was also affected by the presence of nucleotides, as could be inferred from limited tryptic hydrolysis of S-1 (Muhlrad & Hozumi, 1982). The enhancement of tryptophan fluorescence, which was found to be associated with the binding of nucleotides as well as with the intermediate steps of hydrolysis of ATP, was used as a tool to elucidate the mechanism of this myosin-catalyzed process (Bagshaw & Trentham, 1974). However, in order to understand better this process, it would be desirable to study the kinetics of other conformational changes, which take place in well-defined locations in the S-1 segment and are coupled with ATP binding and hydrolysis.

† From the Department of Oral Biology, Hebrew University—Hadassah Faculty of Dental Medicine, Jerusalem 91010, Israel, and the Cardiovascular Research Institute, University of California, San Francisco, California 94143. *Received September 29, 1982.* This research was supported by a Career Investigator Visiting Scientist Award of the American Heart Association and by Grants HL-16683 (U.S. Public Health Service) and CI-8 (American Heart Association).

* Address correspondence to the Hebrew University—Hadassah Faculty of Dental Medicine.

[1] Abbreviations: S-1, myosin subfragment 1; TNP S-1, trinitrophenylated S-1; RLR, reactive lysine residue in S-1; TNBS, 2,4,6-trinitrobenzenesulfonate; AMP-PNP, adenosine 5′-(β,γ-imidotriphosphate); Tes, 2-[[tris(hydroxymethyl)methyl]amino]ethanesulfonic acid; Tris, tris(hydroxymethyl)aminomethane.

0006-2960/83/0422-3653$01.50/0

It was found that the trinitrophenylation of a specific reactive lysyl residue (RLR) per myosin head by trinitrobenzenesulfonate proceeds much faster than that of all the other lysyl residues (Kubo et al., 1960; Muhlrad et al., 1975). The modification of this reactive residue is accompanied by a 2000% increase in Mg^{2+}-mediated and a 90% decrease in K^+- (EDTA) activated ATPase activity (Kitagawa et al., 1961; Fabian & Muhlrad, 1968). The RLR is located in the 27K N-terminus fragment of the heavy chain of S-1 (Mornet et al., 1980; Miyanishi & Tonomura, 1981; Hozumi & Muhlrad, 1981), which also contains the nucleotide "ring" binding site of myosin (Szilagyi et al., 1979). A considerable blue shift was observed in the absorbance spectrum of the trinitrophenyl moiety attached to RLR of S-1 upon addition of ATP or ATP analogues (Muhlrad, 1977). The resulting difference spectra showed a minimum at 365 nm. Changes upon addition of ATP or its analogues were also observed in the circular dichroic spectrum of trinitrophenylated S-1 (Muhlrad, 1977). These spectral alterations indicate that in the vicinity of RLR conformational changes have occurred that are coupled with the binding and hydrolysis of ATP. As these changes were rather substantial, it was convenient to study the kinetics of their appearance, in order to contribute to the elucidation of the detailed mechanism of the myosin-catalyzed ATP hydrolysis.

Materials and Methods

Chemicals. TNBS, ATP, ADP, and ATP–agarose were from Sigma Chemical Co. Chymotrypsin was a Worthington product. AMP-PNP was purchased from ICN. All other chemicals were of reagent grade.

Proteins. Myosin was prepared from back and leg muscles of rabbits according to Tonomura et al. (1966). S-1 was prepared by digestion of myosin filaments with chymotrypsin (Weeds & Taylor, 1975).

Protein Concentrations. Unlabeled myosin and S-1 concentrations were calculated from their absorbances, assuming absorption coefficients $A^{1\%cm}_{280nm}$ of 5.7 and 7.5, respectively. Concentration of trinitrophenylated S-1 was calculated according to the following equation (Muhlrad & Ferencz, 1973):

$$[\text{TNP S-1}]\ (\text{mg/mL}) = (OD_{280nm} - 0.362OD_{345nm})/0.75$$

Light scattering corrections were applied in each case. The molecular weight of S-1 was assumed to be 110K.

Trinitrophenylation of S-1. To 40–45 μM S-1 in 0.1 M Tris-HCl, pH 7.7, was added TNBS to 100 μM final concentration, and it was incubated at 25 °C for 5 min. The resulting mixture was then dialyzed overnight against 12 volumes of 30 mM KCl–10 mM Tes, pH 7.1, with one change at 4 °C. A 10-mL aliquot of the dialyzed preparation was then applied to an affinity column (0.9 × 10 cm) of ATP–agarose [ATP attached to beaded agarose through ribose hydroxyls according to Lamed et al. (1973)], which was equilibrated with 30 mM KCl, 1 mM EDTA, and 10 mM Tes, pH 7.1. The column was washed with 40 mL of equilibrium buffer, which removed denatured S-1, and then with 100 mL of 0.8 mKCl in equilibrium buffer, which eluted active S-1 (Muhlrad et al., 1975). The number of TNP groups attached to S-1 was calculated from the 345-nm absorbance, assuming a $\Delta\epsilon^{M}_{1cm}$ of 1.45×10^4 (Okuyama & Satake, 1960). The purified labeled S-1 generally contained 1.5–1.7 TNP/S-1. Under these conditions 95–98% of the reactive lysyl residue of S-1 was trinitrophenylated.

Absorbance Difference Spectrum. This was measured in matched thermostated cells (15 or 5 °C) of a Cary 118 C spectrophotometer between 300 and 500 nm as described earlier (Muhlrad, 1977). Recording of the spectra was started immediately after mixing of the reagents and was completed within 2 min. There was no change in absorption during this period, since ATP was applied in large excess over S-1.

Fluorescence Spectrum. A Hitachi Perkin-Elmer MPF-4 spectrofluorometer operating at 15 °C in the ratio mode was used for fluorescence measurements. Tryptophan fluorophores of S-1 were excited at 295 nm, and the emission spectrum was recorded.

Transient Kinetic Measurements. These were performed in a Durrum stopped-flow spectrophotometer. The measurements were carried out at 365 nm in a 2-cm light path cell. Constant temperature was maintained by a circulating water bath. Since the absorbance readings at 365 nm obtained with the stopped-flow spectrophotometer were lower than those obtained with the Cary 118C spectrophotometer, the stopped-flow spectrophotometer was calibrated, and the readings were corrected accordingly. The dead time of the apparatus was 3 ms. The concentrations given in each figure represent the final chamber concentrations for the reaction. Each run was repeated at least 4 times; k_{obsd} was calculated from the various traces that were averaged. The maximal difference observed between the individual k_{obsd} values was less than 10%. In both the calculations of rate constant and signal amplitude, the dead time of the instrument, 3 ms, was taken into account, and all values were corrected accordingly.

ATPase Assay. ATPase activities, μmol of P_i (mol of S-1)$^{-1}$ s^{-1}, were calculated from the inorganic phosphate (P_i) content of 2-mL aliquots (aliquots were withdrawn at five consecutive time intervals) of a reaction mixture containing 0.5 μM S-1 or TNP S-1, 1 mM ATP, 30 mM KCl, 4 mM $MgCl_2$, and 10 mM Tes, pH 7.1. The assay was carried out at various temperatures. Reaction conditions were adjusted so that not more than 15% of the ATP was hydrolyzed.

Results

The temperature dependence of the Mg^{2+}-moderated ATPase activity of S-1 and TNP S-1 in the steady state was measured in the range of 5–30 °C (Figure 1). TNP S-1 showed much steeper temperature dependence than normal, nonmodified S-1. The modification caused activation at high temperature and inhibition at low temperature. The crossover point between the two curves was at about 15 °C. The energy of activation derived from the linear Arrhenius plots was 43.6 and 134.5 kJ/mol for S-1 and TNP S-1, respectively.

The steady-state difference absorbance spectrum induced by addition of ATP, ADP, and AMP-PNP in the presence and absence of Mg^{2+} at 15 and 5 °C was recorded between 300 and 500 nm (see Figure 2 for MgATP and MgADP). The minimum of all spectra was found to be at 365 nm, and their shape was substantially the same in all cases. However, the absolute value of $\Delta\epsilon_{365}$ obtained in the presence of ADP was smaller than that for the two other nucleotides (Table I). It should be noted that all values listed corresponded to saturation of binding sites with ligands, as no further change in $\Delta\epsilon_{365}$ was observed upon increasing the concentration of added nucleotides. Neither did $\Delta\epsilon_{365}$ values depend on the extent of trinitrophenylation in the range of 1.2–3 TNP/S-1.

Tryptophan fluorescence of S-1 and TNP S-1 in the absence of nucleotides and in the presence of MgATP, MgADP, and MgAMP-PNP was measured. The emission spectra recorded with and without MgATP are present (Figure 3). It was found that trinitrophenylation of S-1 hardly affected tryptophan fluorescence in the absence of nucleotides (a small 1–2% decrease in fluorescence intensity was observed). On the other hand, the nucleotide-induced tryptophan fluorescence en-

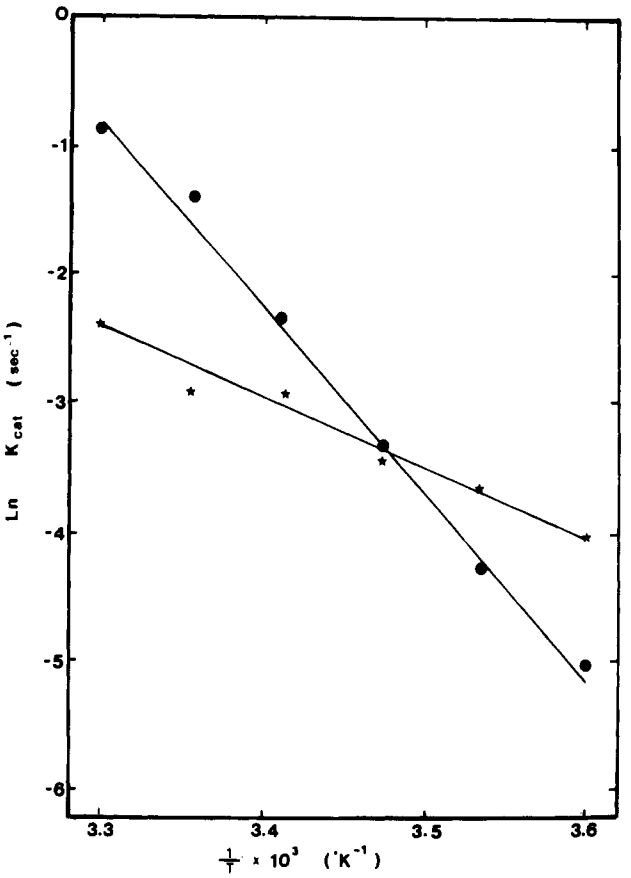

FIGURE 1: Temperature dependence of Mg^{2+}-moderated steady-state ATPase activity of S-1 and TNP S-1: (solid star) S-1; (●) TNP S-1. Conditions for the ATPase assay are as under Materials and Methods. TNP S-1 contained 1.52 TNP/S-1.

Table I: Changes in Molar Extinction Coefficient of TNP S-1 at 365 nm ($\Delta\epsilon_{365}$) upon Addition of ATP and Its Analogues[a]

ligands	$-\Delta\epsilon_{365}$ (M^{-1} cm^{-1}) 15 °C	5 °C
MgATP*	3275	3290
ATP**	3431	3488
MgADP*	2847	2973
ADP**	2713	2954
MgAMP-PNP*	3256	

[a] Conditions: 20 μM TNP S-1 (containing 1.58 TNP/S-1) in 30 mM KCl, 10 mM Tes, and 1 mM ligand, pH 7.1, and either (*) 2 mM $MgCl_2$ or (**) 5 mM EDTA.

hancement was influenced by trinitrophenylation (Table II). A conspicuous difference was recorded in the presence of MgATP: while the fluorescence intensity increased by 30% upon addition of nucleotide in the case of native S-1, only a 12% increase was observed with TNP S-1 under the same conditions. However, the addition of MgADP or MgAMP-PNP induced about the same fluorescence increase in TNP S-1 as in native S-1. The effect of trinitrophenylation on the nucleotide-induced tryptophan fluorescence enhancement did not depend on the number of TNP groups introduced into the S-1 molecule in the range of 1.2–3 TNP/S-1. This indicates that only the TNP that bound to the reactive lysine residue affects the fluorescence change in the presence of MgATP.

The time course of development of the difference in absorption at 365 nm, which is elicited by the addition of nucleotides to TNP S-1, was followed in a stopped-flow spectrophotometer. Several oscilloscope traces of the reaction are shown in Figure 4, where 45 μM ATP was added to 5 μM

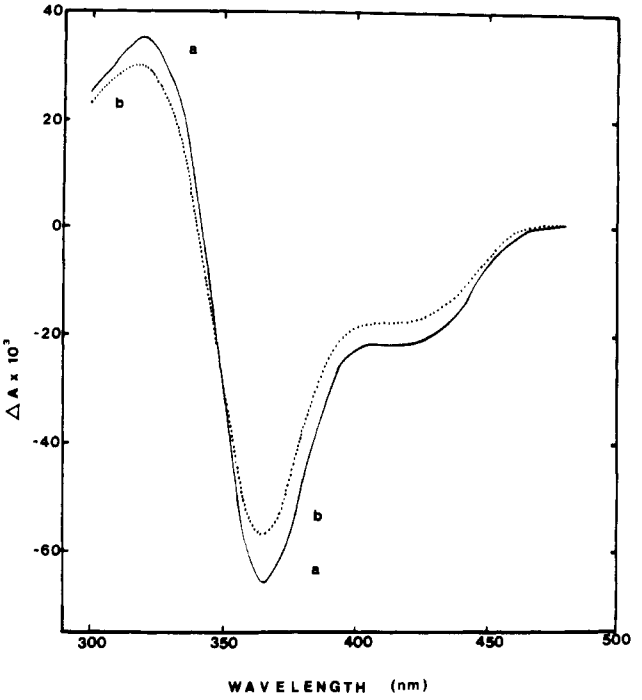

FIGURE 2: Difference spectra of TNP S-1 induced by MgATP and MgADP. Conditions: 1 mM ATP or ADP was added to 20 μM TNP S-1 (containing 1.58 TNP/S-1) in 30 mM KCl, 2 mM $MgCl_2$, and 10 mM Tes, pH 7.1, in thermostated (15 °C) 10-mm matched silica cells of a Cary 118C recording spectrophotometer, with and without nucleotide in the sample and reference positions, respectively. (a) MgATP; (b) MgADP.

Table II: Nucleotide-Induced Tryptophan Fluorescence Enhancement of S-1 at 330 nm (%)[a]

ligands	normal S-1	TNP S-1
MgATP	30.1 ± 1.6	12.2 ± 1.0
MgADP	10.1 ± 0.6	9.9 ± 0.9
MgAMP-PNP	11.3 ± 0.8	11.1 ± 0.9

[a] 100 μM nucleotide was added to 1 μM S-1 or TNP S-1 (containing 1.58 TNP/S-1) in 30 mM KCl, 2 mM $MgCl_2$, and 10 mM Tes, pH 7.1, in a thermostated fluorescence cell. Excitation and emission were at 295 and 330 nm, respectively. Temperature was 15 °C. Each measurement was repeated 4 times.

TNP S-1 in the presence of Mg^{2+} at 15 °C. The time course was fairly reproducible and could be described by a single exponential, which fitted a typical first-order reaction curve with a rate constant of k_{obsd} = 125 s^{-1}. Similar traces, which were all characterized by first-order rate constants, were obtained upon addition of various concentrations of ATP in the presence of Mg^{2+} or EDTA. The rate constants at 15 °C were found to increase with increasing ATP concentration, reaching a plateau at about 75 μM ATP and 100 μM ATP in the presence and absence of Mg^{2+}, respectively (Figure 5). The maximal k_{obsd} values were 210 and 138 s^{-1} for MgATP and ATP, respectively (Figure 5A). In neither case did the k_{obsd} follow a hyperbolic function with respect to ATP concentration, as demonstrated by the nonlinear double-reciprocal plot of these data (Figure 5B).

The experiments described above were also repeated at 5 °C. A similar ATP concentration dependence was obtained at this temperature (Figure 6), with the exception that in this case the plateau value for ATP in the absence of Mg^{2+}, 128 s^{-1}, was higher than in the presence of this divalent cation, 102 s^{-1}. Again, the k_{obsd} values in the presence of Mg^{2+} reached plateau at a lower concentration of ATP than in its absence. The k_{obsd}–[ATP] relation clearly deviated from a hyperbolic

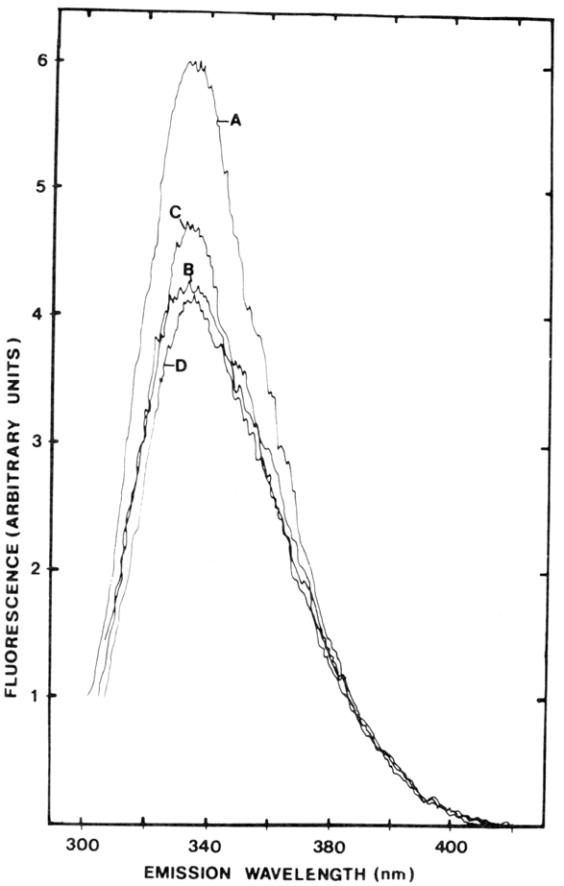

FIGURE 3: Tryptophan fluorescence of S-1 and TNP S-1 in the presence and absence of MgATP. Conditions: 0.1 mM ATP was added to 1 μM S-1 or TNP S-1 (containing 1.58 TNP/S-1) in 30 mM KCl, 2 mM $MgCl_2$, and 10 mM Tes, pH 7.1, in a thermostated (15 °C) fluorescence cell. The solution was excited at 295 nm, and the emission was recorded before and after addition of ATP. (A) S-1 with and (B) S-1 without ATP; (C) TNP S-1 with and (D) TNP S-1 without ATP.

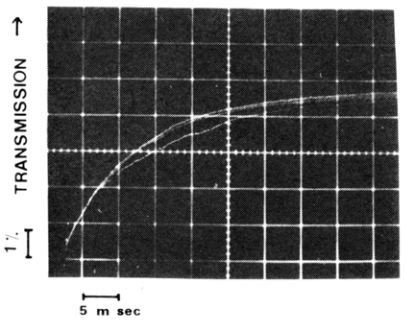

FIGURE 4: Stopped-flow recording of 365-nm absorbance of TNP S-1 when mixed with MgATP. One syringe contained TNP S-1 and the other MgATP. Temperature was 15 °C. Reaction-chamber concentrations: 5 μM TNP S-1 (containing 1.62 TNP/S-1), 45 μM ATP, 2 mM $MgCl_2$, 30 mM KCl, and 10 mM Tes, pH 7.1.

function, as was shown by the nonlinear double-reciprocal plots (Figure 6B).

Oscilloscope traces similar to those obtained with MgATP were obtained also with MgADP. The k_{obsd} values saturated at 0.1 mM MgADP with 150 s^{-1} (Figure 7A). The k_{obsd} values did not fit a hyperbolic function in respect to MgADP concentration (Figure 7B). Addition of ADP in the presence of EDTA also produced an absorbance change at 365 nm (Table I). However, the time course of the development of this change was too rapid to be analyzed accurately in the stopped-flow spectrophotometer, and therefore, k_{obsd} values were not calculated. An absorbance change was also developed

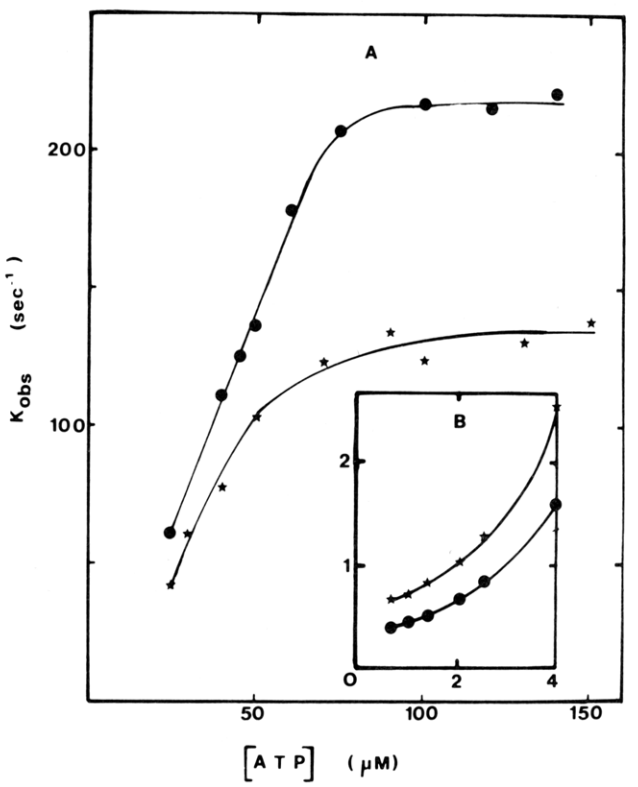

FIGURE 5: Dependence of rate of absorbance change of TNP S-1 on ATP concentration at 15 °C with or without Mg^{2+}: (A) direct plot; (B) double-reciprocal plot of curve in (A); (ordinate) $k_{obsd}^{-1} \times 10^2$ (s); (abscissa) $[ATP]^{-1} \times 10^4$ (M^{-1}). Conditions: 5 μM TNP S-1 (containing 1.62 TNP/S-1), 30 mM KCl, 10 mM Tes, pH 7.1, and either 2 mM $MgCl_2$ (●) or 5 mM EDTA (solid star).

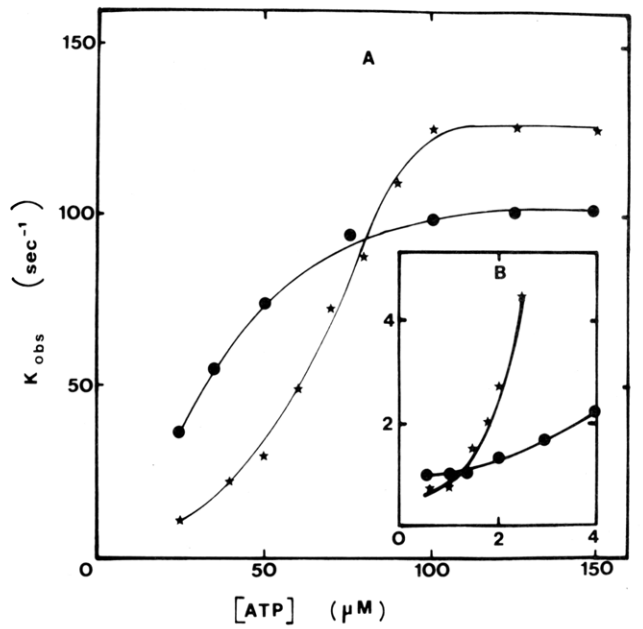

FIGURE 6: Dependence of rate of absorbance change of TNP S-1 on ATP concentration at 5 °C with or without Mg^{2+}: (A) direct plot; (B) double-reciprocal plot of curve in (A); (ordinate) $k_{obsd}^{-1} \times 10^2$ (s); (abscissa) $[ATP]^{-1} \times 10^4$ (M^{-1}). For conditions and symbols, see Figure 5.

by the addition of MgAMP-PNP, a nonhydrolyzable ATP analogue, to TNP S-1 (Table I). The oscilloscope trace could be characterized by a single expotential. The maximal k_{obsd} value was 35 s^{-1}, which was obtained upon addition of 0.1 mM AMP-PNP at 15 °C under the conditions described in Figure 4.

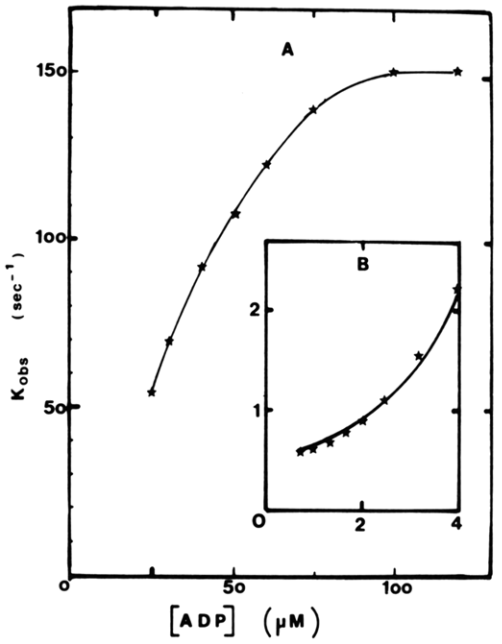

FIGURE 7: Dependence of rate of absorbance change of TNP S-1 on MgADP concentration at 15 °C: (A) direct plot; (B) double-reciprocal plot of curve in (A); (ordinate) $k_{obsd}^{-1} \times 10^2$ (s); (abscissa) $[ADP]^{-1} \times 10^4$ (M^{-1}). Conditions: 5 μM TNP S-1 (containing 1.55 TNP/S-1), 30 mM KCl, 2 mM $MgCl_2$, and 10 mM Tes, pH 7.1.

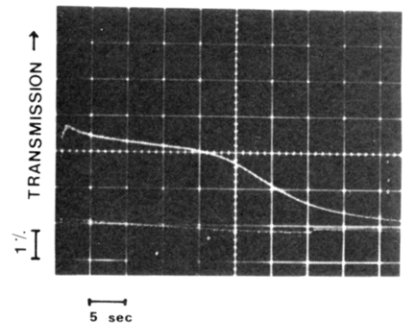

FIGURE 8: Stopped-flow recording of decay of absorbance change induced by MgATP. One syringe contained TNP S-1 and the other MgATP. Temperature was 15 °C. Reaction-chamber concentrations: 10 μM TNP S-1 (containing 1.62 TNP/S-1), 25 μM ATP, 2 mM $MgCl_2$, 30 mM KCl, and 10 mM Tes, pH 7.1.

The entire time course of the hydrolysis of MgATP by TNP S-1 could be followed in the stopped-flow spectrophotometer at 365 nm by using the slowest available time scale of the oscilloscope, viz., 5 s/division (Figure 8). After a fast increase, the oscilloscope trace shows a decay of the difference absorbance at 365 nm. The decay is composed of two phases: a small amplitude decay that follows immediately the appearance of the maximum absorbance and disappears approaching to the steady state and a larger decay correesponding to the exhaustion of ATP. The final level of the decayed difference absorbance corresponds to the value obtained upon addition of MgADP to TNP S-1. The rate constant of the first decay, $k_{decay\,1}$, was 1.2 s^{-1} at 15 °C. The rate constant of the second decay, $k_{decay\,2}$, could be calculated according to Chance (1943) and was found to be 0.115 ± 0.018 and 0.021 ± 0.003 s^{-1} at 15 and 5 °C, respectively.

We measured the ATP concentration dependence of the maximal signal amplitude of TNP S-1 at 365 nm in the stopped-flow spectrophotometer (Figure 9). Virtually identical curves were obtained upon addition of MgATP and ATP both at 15 and 5 °C. A theoretical curve was also calculated by assuming the identical ATP binding site for each S-1 molecule

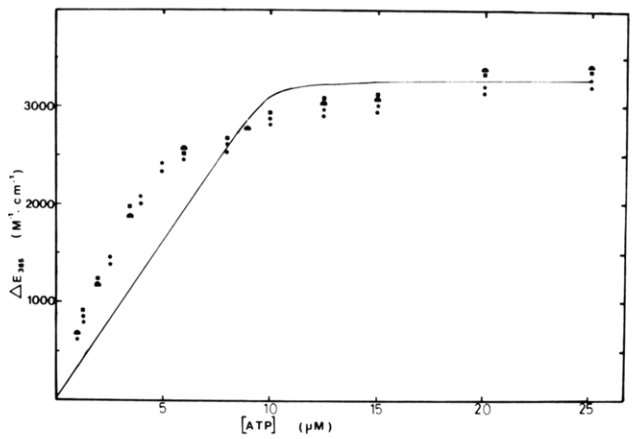

FIGURE 9: Dependence of extent of 365-nm absorbance change of TNP S-1 on ATP concentration with or without Mg^{2+}. The extent of absorbance change was calculated from the maximal amplitude of signal obtained in the stopped-flow spectrophotometer upon addition of ATP to TNP S-1. Conditions: 10 μM TNP S-1 (containing 1.52–1.62 TNP/S-1), 30 mM KCl, and 10 mM Tes, pH 7.1. In addition, 2 mM Mg^{2+} (solid star, ●) or 5 mM EDTA (■, solid half-circle) was also present, and the measurement was carried out at 15 (solid star, ■) or at 5 °C (●, solid half-circle). The continuous line is a theoretical curve drawn for MgATP at 15 °C, assuming one binding site per TNP S-1 and a transient K_M, which controls the height of the absorbance change, 3.13×10^{-8} M. The transient K_M is considered to be $K_M = (k_{decay\,2} + k_{-2})/(K_1 k_2)$. It is assumed that $k_{-2} < k_{decay\,2}$; according to Cardon & Boyer (1978), $k_{-2} = 4 \times 10^{-4}$ s^{-1}. $k_{decay\,2} = 0.115$ s^{-1} at 15 °C (Figure 8). $K_1 = 1.75 \times 10^4$ M^{-1} was calculated from the slope of the MgATP dependence of k_{obsd} (Figure 5); the slope equals $K_1 k_2$ (k_2 is the maximal value of k_{obsd}).

and a transient K_M of 3.13×10^{-8} M for MgATP at 15 °C. The experimental results were significantly different from the theoretical values. The initial slope of the experimental curve was much higher than that of the theoretical one, and it began to curve over at about 70% of its maximum change.

Discussion

In the present paper, we tried to elucidate the effect of a specific chemical modification of S-1, viz., trinitrophenylation of the reactive lysyl residue, on the mechanism of ATP hydrolysis catalyzed by myosin. According to Bagshaw & Trentham (1974) and Taylor (1979) the following scheme adequately describes the hydrolysis of ATP catalyzed by normal myosin or S-1 in the presence of Mg^{2+}:

$$M + ATP \underset{k_{-1}}{\overset{k_1}{\rightleftharpoons}} M\cdot ATP \underset{k_{-2}}{\overset{k_2}{\rightleftharpoons}} M\cdot ATP^* \underset{k_{-3}}{\overset{k_3}{\rightleftharpoons}} M\cdot Pr^{**} \underset{k_{-4}}{\overset{k_4}{\rightleftharpoons}} M\cdot ADP^* \underset{k_{-5}}{\overset{k_5}{\rightleftharpoons}} M\cdot ADP \underset{k_{-6}}{\overset{k_6}{\rightleftharpoons}} M + ADP$$

M·ATP and M·ATP* represent various enzyme–substrate complexes, while M·Pr**, M·ADP*, and M·ADP represent various enzyme–product complexes. The number of stars born by various complexes represents different tryptophan fluorescence intensities. It was shown that the predominant intermediate in the aforementioned hydrolysis scheme of MgATP is an enzyme product complex, M·Pr** (since the transformation of this complex is the rate-limiting step in the overall process). The question arises whether there is any change in the nature of the predominant complex because of the trinitrophenylation of the RLR. It is suggested here that in the kinetic scheme of MgATP hydrolysis catalyzed by TNP S-1 the predominant intermediate is an enzyme–substrate complex, most probably M·ATP* and not M·Pr**. Our assumption is based on the following arguments: (1) According to Miyanishi et al. (1979), the P_i burst is completely abolished

by trinitrophenylation of myosin. The P_i burst, which is associated with the MgATP hydrolysis catalyzed by normal myosin, arises because the actual hydrolysis of ATP (step 3) is much faster than a subsequent step in the mechanisms of ATP hydrolysis (Lymn & Taylor, 1970). Therefore, the abolishment of the P_i burst might mean that either the hydrolysis of ATP became slower or the dissociation of the enzyme–product complex became faster as a consequence of trinitrophenylation of myosin. (2) Addition of ATP in the absence of divalent cations induces essentially the same spectral change in TNP S-1 as MgATP. According to Lymn & Taylor (1970), the rate-limiting step in the EDTA-activated ATPase activity of myosin is the cleavage step. The similar effects of MgATP and ATP on the spectrum of TNP S-1 might suggest that the same step, step 3, is the rate-limiting step both for EDTA- and Mg–ATPase after trinitrophenylation. (3) The same absorbance difference spectrum and fluorescence enhancement are induced in TNP S-1 by MgATP as by its nonhydrolyzable analogue, MgAMP-PNP. In respect of fluorescence enhancement, TNP S-1 differs from nonmodified S-1 where MgAMP-PNP induces less than half of the enhancement of that induced by MgATP. This result has contributed to the recognition that M·Pr** is the predominant complex in the case of normal S-1 (Bagshaw & Trentham, 1974). It has been assumed by the same authors that the complex of MgAMP-PNP with myosin corresponds to M·ATP*. It follows from this assumption that if the addition of MgATP or MgAMP-PNP to TNP S-1 results in complexes with identical spectral properties, then M·ATP* should be the predominant intermediate of the MgATP hydrolysis catalyzed by TNP S-1. Similar conclusions were reached by Stone & Cheung (1976) on the basis that MgATP and MgAMP-PNP induced the same change in the spectral properties of the spin-label attached to SH_1 thiol in trinitrophenylated heavy meromyosin.

It is of interest to find out which step in the Bagshaw–Trentham scheme (Bagshaw & Trentham, 1974) for binding and hydrolysis of ATP by myosin corresponds to the maximum value of k_{obsd}. In the case of normal S-1 (or myosin), both steps 2 and 3 are accompanied by an increase in tryptophan fluorescence [their magnitude being for chymotryptic S-1 10 and 24%, respectively (Weeds & Taylor, 1975)], and according to recently held views (Johnson & Taylor, 1978; Trybus & Taylor, 1982), step 2 is very fast, $k_2 > 1000\ s^{-1}$ and k_3 is the plateau of the observed rate of fluorescence enhancement at high ATP concentration. However, in TNP S-1 catalyzed hydrolysis of MgATP the M·ATP* complex is the predominant intermediate; this means that the rate constant of the transformation (k_3) is relatively slow (in the magnitude of 0.1 s^{-1} at 15 °C) and cannot correspond to the fast k_{obsd}, which has the magnitude of 100 s^{-1}. It follows from these facts that when MgATP is added to TNP S-1, the maximal rate of absorbance change at 365 nm represents k_2. The k_2 of TNP S-1 is about 1 magnitude smaller than that of normal S-1 at 15 °C.

The dependence of the observed rate constant on MgATP, ATP, or MgADP concentration deviated from a hyperbolic behavior. To understand this behavior, one has to consider the binding of MgATP by myosin according to the Bagshaw & Trentham (1974) scheme. The first step of MgATP binding in this scheme is a rapid equilibrium, which is followed by a relatively slower izomerization step. This is true only if k_{obsd} reaches plateau at high nucleotide concentration, and the concentration dependence of k_{obsd} is hyperbolic. Deviation from hyperbolic behavior can be expected if the step immediately preceding the spectral change is not in a rapid equilibrium. Deviation from the hyperbola was observed recently also with normal S-1, and it was suggested to be derived from a three-step nucleotide binding process, in which the first rapid equilibrium step is followed by two slower, essentially irreversible isomerization steps (Chock et al., 1979; Johnson & Taylor, 1978; Trybus & Taylor, 1982). This might be true also for the nucleotide binding of TNP S-1, and in this case, virtually the whole absorbance change should be associated with the last isomerization step. However, the deviation from hyperbolic behavior may also be due to heterogeneity of the TNP S-1 population, as was indicated by studying the ATP concentration dependence of the signal amplitude.

The analysis of the MgATP or ATP concentration dependence of the amplitude of the absorbance change induced in TNP S-1 indicates heterogeneity of the MgATP (or ATP) binding sites, since the theoretically computed binding curve, which assumed one identical ATP binding site for each TNP S-1 molecule, was significantly different from the experimental one. As it is assumed that each S-1 molecule has one high affinity ATP binding site (Young, 1967), it follows that the TNP S-1 molecules belong to more than one class with respect to ATP binding. Similar findings were obtained earlier regarding ADP binding by TNP S-1 (Muhlrad, 1977). Furthermore, Miyanishi et al. (1979) showed that RLR was trinitrophenylated only in one of the myosin heads, when the reaction was carried out in the presence of magnesium pyrophosphate. Finally, our previous results (Hozumi & Muhlrad, 1981) concerning limited tryptic hydrolysis of S-1 trinitrophenylated in the presence and in the absence of magnesium pyrophosphate again indicated heterogeneity of the myosin heads after trinitrophenylation.

An interesting feature of the kinetics of absorbance change associated with nucleotide binding by TNP S-1 is its relative insensitivity to the presence of Mg^{2+}. This is also true for the nucleotide concentration dependence of the signal amplitude. These findings indicate that the affinities of ATP and MgATP toward TNP S-1 are essentially identical, and the same seems to be true for ADP and MgADP as well [see Muhlrad (1977) for the dependence of $\Delta\epsilon_{365}$ on the concentration of ADP and MgADP]. On the other hand, the response of normal, nonmodified S-1 to nucleotides greatly depends on the presence of Mg^{2+}; Mg^{2+} increases the fluorescence enhancement induced by both ATP and ADP (Werber et al., 1972), and the affinity of MgADP toward heavy meromyosin is much higher than that of ADP (Malik et al., 1972) even if we consider that at pH 7.0 and low ionic strength H·ADP binds to myosin fairly tightly (Martonosi & Kielly, 1969). It thus seems that the trinitrophenylation of RLR essentially abolishes the difference in sensitivity toward ATP and MgATP in the nucleotide binding site of S-1.

A decay of the difference absorbance was observed following the maximal spectral change after the addition of MgATP to TNP S-1. This decay is composed of two parts: a fast pre-steady-state decay with a small amplitude and a second larger decay that appears later and corresonds to the exhaustion of ATP in the reaction mixture. The analysis of the first fast decay according to Bagshaw & Trentham (1974) contributes to the determination of the rate-limiting step in the hydrolysis of MgATP by TNP S-1. In this hydrolysis scheme, there are three potential rate-limiting steps: k_3, k_4, and k_6. All the others are assumed to be fast. Since no significant amount of M·Pr** can be found in the steady-state complex, it is assumed that $k_3 \ll k_4$. The analysis of the scheme according to Bagshaw & Trentham (1974) gives $k_{cat} = k_3k_6/(k_3 + k_6)$,

$k_{decay\,1} = k_3 + k_6$, $[M{\cdot}ATP^*]_{steady\ state} = k_6[M_0]/(k_3 + k_6)$, and $[M{\cdot}ADP^*]_{steady\ state} = k_3[M_0]/(k_3 + k_6)$. $[M_0]$ is the total TNP S-1 concentration. According to our results, k_{cat} and $k_{decay\,1}$ at 15 °C are 0.04 and 0.72 s^{-1}, respectively. Since $k_{decay\,1}$ is at least 1 magnitude higher than k_{cat}, therefore, k_3 cannot be equal to k_6. If $k_3 > k_6$, then $[M{\cdot}ATP^*]_{steady\ state}$ would be low and the first decay would have a considerable amplitude, which are contrary to the present findings. It follows that $k_3 < k_6$, and k_3 is the significant rate-limiting step in the hydrolysis of MgATP. On the basis of the above equations, one can estimate the rate constants and the percentual composition of the steady-state complex at 15 °C: k_3 and k_6 are 0.042 and 0.68 s^{-1}; M·ATP* and M·ADP* are 94 and 6% of the steady-state complex, respectively. It should be noted, however, that these values are rather crude estimates since the rate constant of the first decay cannot be evaluated accurately due to its very small amplitude.

The steady-state rate constant of TNP S-1 shows a marked temperature dependence, and its activation energy, 135 kJ/mol, is 3 times as high as that of normal S-1. It should be noted in this respect that increased activation energy was found also after modification of SH groups of myosin and S-1 (Levy et al., 1962; Sleep et al., 1981). However, the Arrhenius plot of ATPase activity of TNP S-1 was linear in the whole temperature range studied, unlike that of the SH-modified S-1, which showed a considerable curvature at low temperature (Levy et al., 1962; Sleep et al., 1981). It should be mentioned, however, that Morales & Hotta (1960) obtained a linear Arrhenius plot after thiol modification. The values of activation energy obtained in our studies for normal S-1 are in good agreement with those published earlier (Levy et al., 1962; Baruch & Moos, 1971; Sleep et al., 1981).

Trinitrophenylation of the RLR of S-1 did not affect tryptophan fluorescence in spite of the fact that the spectral properties of the TNP moiety attached to lysine (absorption peak being at 345 nm, near the maximum of fluorescence emission of tryptophan) make it a putative quencher of tryptophan fluorescence. The apparent lack of energy transfer (quenching) between the moieties indicates that RLR is located at a considerable distance from any tryptophan in the three-dimensional structure of the myosin head. Addition of MgATP increases by more than 30% the fluorescence intensity of normal S-1 prepared by chymotryptic digestion (Weeds & Taylor, 1975) while MgAMP-PNP or MgADP give less than half of this fluorescence enhancement. The nonhydrolyzable nucleotides induce the same fluorescence enhancement in TNP S-1 as in normal S-1. However, the MgATP-induced tryptophan fluorescence enhancement is considerably reduced as a consequence of trnitrophenylation of S-1, and the fluorescence emission is about on the same level as that observed upon addition of MgAMP-PNP. We assume that the loss of the greater part of the MgATP-induced fluorescence enhancement is caused by the fact that M·ATP* and not M·Pr** is the predominant complex in the TNP S-1 catalyzed hydrolysis of MgATP; and therefore, the concentration of M·Pr**, which is characterized by a high fluorescence level (Bagshaw & Trentham, 1974), is relatively low in the steady state.

The observed lack of actin activation of the MgATP hydrolysis catalyzed by trinitrophenylated myosin (Fabian & Muhlrad, 1968) could be also explained by the change in the predominant complex upon trinitrophenylation. Actin activates the ATPase activity of normal myosin by accelerating the transformation of the steady-state complex M·Pr** to M·ADP* but does not affect the actual hydrolysis of ATP: the M·ATP*–M·Pr** transformation (Taylor, 1979). As M·ATP* is the predominant complex in the TNP myosin catalyzed hydrolysis of MgATP, it is quite natural that actin, which does not influence the rate of transformation of this complex, will not affect the rate of the overall hydrolysis of ATP either.

In conclusion, the present study shows that both substrate binding and catalytic characteristics of S-1 are thoroughly affected by trinitrophenylation of RLR. Binding and hydrolysis of MgATP by TNP S-1 are similar to binding and hydrolysis of ATP (in the absence of divalent cations) by normal S-1. This means that the predominant intermediate in the kinetic scheme of the hydrolysis of MgATP by TNP S-1 is an enzyme–substrate complex instead of an enzyme–product complex, which is the case with normal unmodified S-1.

Acknowledgments

I am indebted to Professor M. F. Morales for his continued interest in the work, for helpful discussions, and for his kind hospitality. Thanks are also due to Drs. M. M. Werber and J. Borejdo for valuable suggestions during preparation of the manuscript.

Registry No. ATPase, 9000-83-3; MgATP, 1476-84-2; MgADP, 7384-99-8; MgAMP-PNP, 69977-25-9; ATP, 56-65-5; ADP, 58-64-0.

References

Bagshaw, C. R., & Trentham, D. R. (1974) *J. Biochem. (Tokyo) 141*, 331–349.
Baruch, W. W., & Moos, C. (1971) *Biochim. Biophys. Acta 234*, 183–189.
Cardon, J. W., & Boyer, P. D. (1978) *Eur. J. Biochem. 92*, 443–448.
Chance, B. (1943) *J. Biol. Chem. 151*, 553–565.
Cheung, H. C. (1969) *Biochim. Biophys. Acta 194*, 478–485.
Chock, S. P., Chock, P. B., & Eisenberg, E. (1979) *J. Biol. Chem. 254*, 3236–3243.
Fabian, F., & Muhlrad, A. (1968) *Biochim. Biophys. Acta 162*, 596–603.
Hozumi, T., & Muhlrad, A. (1981) *Biochemistry 20*, 2945–2949.
Johnson, K. A., & Taylor, E. W. (1978) *Biochemsitry 17*, 3432–3442.
Kitagawa, S., Yoshimura, J., & Tonomura, Y. (1961) *J. Biol. Chem. 236*, 902–906.
Kubo, S., Tokura, S., & Tonomura, Y. (1960) *J. Biol. Chem. 233*, 2835–2839.
Lamed, R., Levin, Y., & Oplatka, A. (1973) *Biochim. Biophys. Acta 305*, 163–171.
Levy, H. M., Sharon, N., Ryan, E. M., & Koshland, D. E., Jr. (1962) *Biochim. Biophys. Acta 56*, 118–126.
Lymn, R. W., & Taylor, E. W. (1970) *Biochemistry 9*, 2975–2983.
Malik, M. N., Marchioli, L., & Martonosi, A. (1972) *Arch. Biochem. Biophys. 153*, 147–155.
Martonosi, A., & Kielly, B. (1969) *Biochim. Biophys. Acta 172*, 158–170.
Miyanishi, T., & Tonomura, Y. (1981) *J. Biochem. (Tokyo) 89*, 831–839.
Miyanishi, T., Inoue, A., & Tonomura, Y. (1979) *J. Biochem. (Tokyo) 85*, 747–753.
Morales, M. F., & Hotta, K. (1960) *J. Biol. Chem. 235*, 1979–1986.
Morita, F. (1967) *J. Biol. Chem. 242*, 4501–4506.
Mornet, D., Pantel, P., Bertrand, R., Audemard, E., & Kassab, R. (1980) *FEBS Lett. 117*, 183–188.

Muhlrad, A. (1977) *Biochim. Biophys. Acta 493*, 154–166.
Muhlrad, A., & Ferencz, K. (1973) *Physiol. Chem. Phys. 5*, 13–26.
Muhlrad, A., & Hozumi, T. (1982) *Proc. Natl. Acad. Sci. U.S.A. 79*, 958–962.
Muhlrad, A., Lamed, R., & Oplatka, A. (1975) *J. Biol. Chem. 250*, 175–181.
Okuyama, T., & Satake, K. (1960) *J. Biochem. (Tokyo) 47*, 454–462.
Seidel, J. C., Chopek, M., & Gergely, J. (1970) *Biochemistry 9*, 3265–3272.
Sleep, J. A., Trybus, K. M., Johnson, K. A., & Taylor, E. W. (1981) *J. Muscle Res. Cell Motil. 2*, 373–399.
Stone, D. B., & Cheung, P. H. (1976) *Biophys. J. 16*, A46.
Szilagyi, L., Balint, M., Sreter, F. A., & Gergely, J. (1979) *Biochem. Biophys. Res. Commun. 87*, 936–945.
Taylor, E. W. (1979) *CRC Crit. Rev. Biochem. 6*, 103–164.
Tonomura, Y., Appel, P., & Morales, M. F. (1966) *Biochemistry 5*, 515–521.
Trybus, K. M., & Taylor, E. W. (1982) *Biochemistry 21*, 1284–1294.
Weeds, A. G., & Taylor, R. S. (1975) *Nature (London) 257*, 54–56.
Werber, M. M., Szent-Gyorgyi, A. G., & Fasman, A. D. (1972) *Biochemistry 11*, 2872–2883.
Young, M. (1967) *J. Biol. Chem. 242*, 2790–2792.

Interaction of Apolipoprotein B from Human Serum Low-Density Lipoprotein with Egg Yolk Phosphatidylcholine and Cholesterol†

Subhash Dhawan and Jacqueline A. Reynolds*

ABSTRACT: Binary and ternary complexes of apolipoprotein B (apo B) with egg yolk lecithin and with lecithin plus cholesterol have been formed from detergent–lipid–protein mixed micelles. These particles appear to be spherical by negative-stain electron microscopy and contain 510000 g of protein (2 mol of apo B) complexed with apparent maximum molar ratios of 780:2 (egg yolk lecithin:apo B) and 1300:280:2 (egg yolk lecithin:cholesterol:apo B). The secondary structure as reflected in the circular dichroic spectra is similar to that of holo-LDL_2 when only lecithin is bound, but is significantly altered when cholesterol is also present in the complex, suggesting that the molecular organization of the ternary complex formed in the absence of neutral lipids is significantly different from that of the native lipoprotein. A part of the protein (presumably uncharged) has to be incorporated with the lipid acyl chains in a hydrophobic "core" of the spherical particle. However, the relative amounts of apo B exposed to the aqueous solvent and to the hydrophobic interior of the recombined particles depend on the lipid content and also appear to differ from those in LDL_2. The results suggest that the manner in which apo B folds is continuously variable, a result consistent with its ability to bind varying amounts of lipid in vivo.

Apolipoprotein B (apo B)[1] is the core protein common to very low density and low-density serum lipoproteins (VLDL and LDL, respectively) and is present in these water-soluble complexes in a constant mass of 510000 g—equivalent to two polypeptide chains per particle (Schumaker, 1973; Fisher et al., 1975; Tanford & Reynolds, 1979). Apo B forms complexes in vivo with 5–20 times its own mass of various lipids and perhaps more importantly can vary its binding capacity as the lipid content is altered during intravascular catabolism of VLDL to the ultimate product, LDL_2.

One approach to understanding how the core protein, apo B, and the naturally occurring lipids combine and organize themselves into a water-soluble structure is to investigate systematically the binding of specific lipid moieties to the purified protein and the effect of this interaction on protein structure. We have used this approach previously (Watt & Reynolds, 1981) and in this study have extended our previous investigations of the binary apo B–EYL complex to the ternary apo B–EYL–cholesterol complex.

Experimental Procedures

Materials

All materials used in this study were standard reagent grade unless otherwise specified. Sodium dodecyl sulfate was BDH Chemical Corp. specially pure grade purchased from Gallard Schlesinger. Sephacryl S500 and Sepharose CL-4B were products of Pharmacia Fine Chemicals. Egg yolk lecithin used in this study was from Lipid Products and contained less than 0.5% contamination by fatty acid or lysolecithin as determined by high-pressure liquid chromatography. Cholesterol was purchased from Applied Sciences, and [^{14}C]cholesterol was from Amersham-Searle.

Methods

Preparation of Holo-LDL_2. Holo-LDL_2 (d = 1.02–1.05 g/cm^3) was isolated from fasting, normal human volunteers by centrifugal flotation by employing the procedures described in detail by Steele & Reynolds (1979). After isolation, the two free sulfhydryls per 250000 g of protein were alkylated

† From the Department of Physiology, Duke University Medical Center, Durham, North Carolina 27710. *Received January 31, 1983.* This work was supported by U.S. Public Health Service Grant HL 30049 and the Whitehead Medical Research Institute.

[1] Abbreviations: LDL, human serum low-density lipoprotein; VLDL, human serum very low density lipoprotein; apo B, apolipoprotein B; EYL, egg yolk phosphatidylcholine; Tes, *N*-[tris(hydroxymethyl)methyl]-2-aminoethanesulfonic acid.

0006-2960/83/0422-3660$01.50/0